

Reinforcement-Learning-Based Resource Allocation in Fog Radio Access Networks for Various IoT Environments

Almuthanna T. Nassar, and Yasin Yilmaz, *Member, IEEE*

Electrical Engineering Department, University of South Florida, Tampa, FL 33620, USA

E-mails: {atnassar@mail.usf.edu; yasin@usf.edu}

Abstract—Fog radio access network (F-RAN) has been recently proposed to satisfy the low-latency communication requirements of Internet of Things (IoT) applications. We consider the problem of sequentially allocating the limited resources of a fog node to a heterogeneous population of IoT applications with varying latency requirements. Specifically, for each service request it receives in time, fog node needs to decide whether to serve that user locally to provide it with low-latency communication service or to refer it to the cloud control center to keep valuable fog resources available for future users with potentially higher utility to the system (i.e., lower latency requirement). We formulate the problem as a Markov Decision Process (MDP) in two alternative formulations: infinite-horizon MDP (IH MDP) and finite-horizon MDP (FH MDP). In both IH and FH formulations, we present the optimal solution, known as the optimal policy, through Reinforcement Learning (RL). The optimal policies in both cases are learnt from the IoT environment using different RL methods. The significant advantage of the proposed RL methods over the straightforward approach of deciding based on a fixed threshold of utility is that the RL methods quickly learn the optimal decision thresholds from the IoT environment, and thus always achieve the best possible performance regardless of the environment. They strike the right balance between the two conflicting objectives, maximize the average total served utility vs. minimize the fog node's idle time. Extensive simulation results for various IoT environments corroborate the theoretical underpinnings of the proposed RL methods.

Index Terms— IoT Communications, Fog RAN, 5G Cellular Networks, Low-Latency Communications, Resource Allocation, Markov Decision Process, Reinforcement Learning.

I. INTRODUCTION

There is an ever-growing demand for wireless communication technologies due to several reasons such as the increasing popularity of Internet of Things (IoT) devices, the widespread use of social networking platforms, the proliferation of mobile applications, and the current lifestyle that has become highly dependent on technology in all aspects. It is expected that the number of connected devices worldwide will reach three times the global population in 2021 with 3.5 devices per capita. However, in some regions, such as North America, the number of connected devices is projected to reach about 13 devices per capita by 2021, which makes the massive IoT a very common concept. This trend of massive IoT will generate an annual global IP traffic of 3.3 zettabytes by 2021, which corresponds to 3-times the traffic in 2016 and 127-times the traffic in 2005, in which wireless and mobile devices will account for the 63% of this forecast [1]. This unprecedented demand for mobile data services makes it unbearable for service providers with the current third generation (3G) and fourth generation (4G) networks to keep pace with it [2].

The design criteria for fifth generation (5G) wireless communication systems will include providing ultra-low latency, wider coverage, reduced energy usage, increased spectral efficiency, more connected devices, improved availability, and very high data rates of multi giga-bit-per-second (Gbps) everywhere in the network

including cell edges [2]. Several radio frequency (RF) coverage and capacity solutions are proposed to fulfill the goals of 5G. Millimeter-wave (mm-wave) frequency range is likely to be utilized in 5G because of the spacious bandwidths available in these frequencies for cellular services [3, 4]. Massive multi-input-multi-output (MIMO) is potentially involved for excellent spectral efficiency and superior energy efficiency [5, 6].

To cope with the growing number of IoT devices and the increasing amount of traffic for better user satisfaction, cloud radio access network (C-RAN) architecture is suggested for 5G, in which a powerful cloud controller (CC) with pool of baseband units (BBU) and storage pool supports large number of distributed remote radio units (RRU) through high capacity fronthaul links [7, 8]. The C-RAN is characterized by being clean as it reduces energy consumption and improves the spectral efficiency due to the centralized processing and collaborative radio [9]. However, in light of the massive IoT applications and the corresponding generated traffic, C-RAN structure places a huge burden on the centralized CC and its fronthaul, which causes more delay due to limited fronthaul capacity and busy cloud servers in addition to the large transmission delays [10, 11].

A. F-RAN and Heterogeneous IoT

This latency issue in C-RAN becomes critical for IoT applications that cannot tolerate such delays. And that is the reason fog radio access network (F-RAN) is introduced in 5G, where fog nodes (FN) are not only limited to perform RF functionalities but also empowered with caching, signal processing and computing resources [12, 13]. This makes FNs capable of independently delivering network functionalities to end users at the edge without referring to the cloud to tackle the low-latency needs.

IoT applications have various latency requirement. Some applications are more delay-sensitive than others, while some can tolerate larger delays. Hence, especially in a heterogeneous IoT environment with various latency needs, FN must allocate its limited and valuable resources in a smart way. In this work, we present a novel framework for resource allocation in F-RAN for 5G to guarantee the efficient utilization of limited FN resources while satisfying the low-latency requirements of IoT applications [14-16].

B. Literature Review

For the last several years, 5G and IoT related topics have been of great interest to many researchers in the wireless communications field. Recently, a good number of works in the literature focused on achieving low latency for IoT applications in 5G F-RAN. Cooperative computing and resource allocation for achieving ultra-low latency in F-RAN has been studied in [17-22]. Instead of using a centralized server, edge mesh computing paradigm is proposed in [17], where the decision-making tasks are distributed among the edge devices. The authors in [18, 21] considered heterogeneous F-RAN structures including, small cells and macro base stations, and provided an algorithm for selecting the F-RAN nodes to serve with proper heterogeneous resource allocation. Content fetching is used in [7, 19] to maximize the delivery rate when the requested content is available

in the cache of fog access points. In [23], cloud predicts users' mobility patterns and determines the required resources for the requested contents by users, which are stored at cloud and small cells. The work in [20] addressed the issue of load balancing in fog computing and used fog clustering to improve user's quality of experience. The congestion problem, when resource allocation is done based on the best signal quality received by the end user, is highlighted in [24, 25]. [24] provided a solution to balance the resource allocation scheduling among remote radio heads by achieving an optimal downlink sum-rate, while [25] offered an optimal solution based on reinforcement learning to balance the load among evolved nodes for the arrival of machine-type communication devices. To reduce latency, soft resource reservation mechanism is proposed in [26] for uplink scheduling. To ease the user mobility challenge and reduce the application response time [27] presented an algorithm that works with the smooth handover scheme and suggested scheduling policies. Radio resource allocation strategies to optimize spectral efficiency and energy efficiency while maintaining a low latency in F-RAN are proposed in [28]. With regard to learning for IoT, [29] provided a comprehensive study about the advantages, limitations, applications, and key results relating to machine learning, sequential learning, and reinforcement learning. Multi-agent reinforcement learning was exploited in [30] to maximize network resource utilization in heterogeneous network by selecting the radio access technology and allocating resources for individual users. The model-free reinforcement learning approach is used in [31] to learn the optimal policy for user scheduling in heterogeneous networks to maximize the network energy efficiency.

C. Contributions

With the motivation of satisfying the low-latency requirements of heterogeneous IoT applications through F-RAN, we provide a novel framework for allocating limited resources to users, that guarantees efficient utilization of limited FN resources. In this work, we develop Markov Decision Process (MDP) formulations for the considered resource allocation problem and provide Reinforcement Learning (RL) based algorithms for learning optimum decision-making policies adaptive to the IoT environment. Specifically, our contributions can be listed as:

1. Developing MDP formulations for finite horizon and infinite horizon scenarios.
2. Providing analytical solution for the finite horizon MDP using dynamic programming.
3. Characterization of solution for the infinite horizon MDP and showing how to implement optimal policies using RL.

The remainder of the paper is organized as follows. Section II introduces the system model. The MDP formulation of the resource allocation problem is given in Section III. We derive the optimum policies and discuss the related algorithms in Section IV. Simulation results are presented in Section V. Finally, we conclude the paper in Section VI.

II. SYSTEM MODEL

We consider the F-RAN structure shown in Fig. 1, in which fog-nodes (FNs) are connected through the fronthaul to the cloud controller (CC), where a massive computing capability, centralized baseband units (BBUs) and cloud storage pooling are available. To overcome the challenge of the increasing number of IoT devices and low-latency applications, and to ease the burden on the fronthaul and the cloud, FNs are empowered to deliver network functionalities at the edge. Hence, they are equipped with caching capacity, computing and signal processing capabilities. These resources are limited and therefore, need to be utilized efficiently. IoT applications have various levels of latency requirement; some users are delay-tolerant such as a smart phone used

for browsing, while others can be classified as low-latency users like an autonomous car. So, it is sensible for the FN to give higher priority to the request from autonomous car since it has higher utility to the network. On the other hand, a lower priority level will be assigned to the smart phone request of less utility. Hence, we define utility to be equal to the priority level of a user, which is directly proportional to its level of latency requirement.

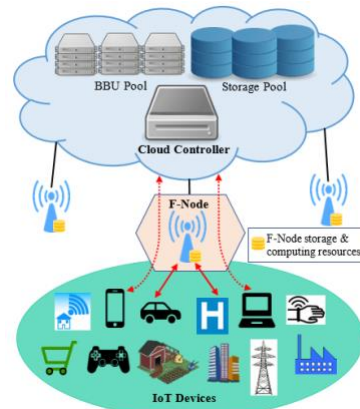


Fig. 1. Fog-RAN System Model

An end user attempts to access the network by sending a request to the nearest FN. The FN checks the priority level and then takes a decision whether to serve the user locally at the edge using its own computing and processing resources or refer it to the cloud. We consider the FN's computing and processing capacity is limited to N slots. Zooming in, we partition the time into very small time-steps $t = 1, 2, \dots$ and consider a high-rate sequential arrival of users, one user at a time-step. We assume that the time required to fill the slots is much shorter than the average user serving time. FNs should be smart to learn how to decide (serve/refer to the cloud) for each user (i.e., how to allocate its limited resources), in a way to achieve the objective of maximizing the average total utility of served users over time and minimizing its idle (no-service) time.

One approach to deal with this resource allocation problem is to apply a fixed threshold on the user's priority to be served at the FN level. For instance, if we consider ten different priorities $\{1, 2, 3, \dots, 10\}$ of IoT applications where 10 represents the highest priority user and 1 is for the lowest priority. Then, we can define a threshold rule, such as "serve if priority greater than 5". However, such a policy is suboptimum since the FN will be waiting for a user to satisfy the threshold, which will increase the idle time. The main drawback of this policy is that it cannot adapt to the dynamic IoT environment to achieve the objective. For instance, when the user priorities are almost uniformly distributed, a very selective policy with a high threshold will stay idle most of the time, whereas an impatient policy with a low threshold will in general obtain a low average served utility. A mild policy with threshold 5 may in general perform better than the extreme policies, yet it will not be able to adapt to a dynamic IoT environment. A better solution for the F-RAN resource allocation problem is to use reinforcement learning (RL) techniques which can continuously learn the environment and adapt the decision rule accordingly.

III. RL PROBLEM FORMULATION

RL can be thought as the third paradigm of machine learning (ML) considering the other two paradigms, supervised ML and unsupervised ML. The key point in RL is that FN learns about the IoT environment by interaction and then adapts to it. FN gains rewards from the environment for every action it takes, and once the optimum policy of actions is learned, FN will maximize its average rewards and achieve the objective. For an access request from a user with utility u_t , at time t , if the FN decides to take the action $a_t = \text{serve}$ which means to serve

the user at the edge, then it will gain its utility value as a reward $r_{t+1} = u_t$ and one slot of the FN's resources will be occupied. Otherwise for the action $a_t = \text{wait}$ which means to refer the current user to the cloud and wait for a better future utility, then the FN will maintain its resources but it will get a reward $r_{t+1} = -\eta$ where η is the penalty of waiting, whose role is to encourage less idle time. We define the state S of the FN at any time as the number of available slots at that time, where future state is independent of past states given the current state, i.e., Markov state. Hence, we formulate the Fog-RAN resource allocation problem in two forms of sequential Markov decision process (MDP): the infinite-horizon (IH) MDP and the finite-horizon (FH) MDP. The IH case represents a soft constraint for filling time through a waiting penalty. More penalties will be collected for more wait-actions; thus, the FN is encouraged somehow to serve, however it will decide to wait if waiting might maximize the expected future rewards. In FH case, there is a hard constraint on the FN in terms of the value of time as it must terminate within a limited time T_f regardless whether the N slots are filled or not. This means that the MDP will terminate either at the termination time T_f or before if all slots are filled earlier.

A. Infinite-Horizon MDP

For the considered sequential MDP problem, the utility of a user is denoted with u which has the same value of user's priority level, e.g., $u \in \{1, 2, 3, \dots, 10\}$. We consider that the FN has N slots of serving resources. In the IH case, for an FN of N slots, there are $N + 1$ states, $S \in \{S_0, \dots, S_n, \dots, S_N\}$ where n denotes the number of occupied slots. So, at the initiation time $t = 0$, all slots are available, $n = 0$, hence the initial state of FN is S_0 , while S_N represents the terminal state with all slots are occupied. At every time step t , the FN receives a request from a user of utility u_t , and FN takes an action $a_t \in \{\text{serve}, \text{wait}\}$. Based on its decision, the FN receives an immediate reward $r_{t+1} = \{u_t, -\eta\}$ and it moves to a successor state (the following state or the current state). The IH MDP terminates at time T when the terminal state S_N is reached. State transitions for the 2-slot case ($N = 2$) are shown in Table 1. Being at state S , and taking the action a will result in getting an immediate reward r and moving to the successor state S' . All possible combinations of states and actions are shown in Table 1.

TABLE 1
STATE TRANSITIONS FOR $N = 2$

S	a	r	S'
S_0	Wait	$-\eta$	S_0
S_0	Serve	u	S_1
S_1	Wait	$-\eta$	S_1
S_1	Serve	u	S_2

We can also draw the dynamics of the tabular IH MDP using a state transition graph as shown in Fig. 2, in which non-terminal states and terminal states are represented by open circles and squares, respectively, and labeled by the states names, solid circles represent actions, and arrows show the transitions with corresponding rewards.

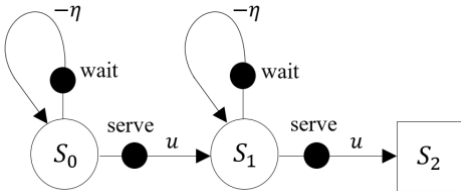


Fig. 2. State transition graph for IH MDP with $N = 2$. States are labeled by S_n where n is the number of filled slots.

We define the return G_t as the total discounted rewards received from time t till termination, $G_t = \sum_{j=0}^{\infty} \gamma^j r_{t+j+1}$, where $\gamma \in [0, 1]$ is

the discount factor which represents the weight or importance of future rewards with respect to the immediate reward, and after termination $r = 0$. $\gamma = 0$ ignores future rewards, whereas $\gamma = 1$ means that future rewards are of the same importance as the immediate rewards.

Starting at the initial state $S = S_0$, the objective is to find the optimal decision policy which maximizes the expected initial return $E[G_0]$. The state-value function $V(S_0)$, where $V(S)$ is shown in (1), is equal to the objective function $E[G_0]$. $V(S)$ represents the long-term value of being in the state S in terms of the expected return which can be collected starting from this state onward till termination. Based on the definition the terminal state has a zero value since no reward can be collected from that state. The state value can be viewed also in two parts: the immediate reward from the action taken and the discounted value of the successor state where we end in. Similarly, we define the action-value function $Q(S, a)$ as the expected return that can be achieved after taking the action a at state S , as shown in (2). The action value function tells how good it is to take a particular action at a given state. The expressions in (1) and (2) are known as the Bellman expectation equations for state value and action value, respectively [32],

$$V(S) = E[G_t|S] = E[r_{t+1} + \gamma V(S')|S], \quad (1)$$

$$Q(S, a) = E[G_t|S, a] = E[r_{t+1} + \gamma Q(S', a')|S, a], \quad (2)$$

where a' denotes the successor action at the successor state S' . Since (1) shows the relationship between the value of a state and its successor states, similarly for the value of an action in (2), it is useful to show the dynamics of the MDP in a backup diagram, as shown in Fig. 3 for the FN with $N = 2$. In the backup diagram, unlike transition graph, the states are not necessarily distinct at each level, i.e., a state might be the same as its successor. From the same figure we can see that the minimum termination time required to reach the terminal state S_2 is $T = 2$. Note that early termination does not necessarily maximize the return.

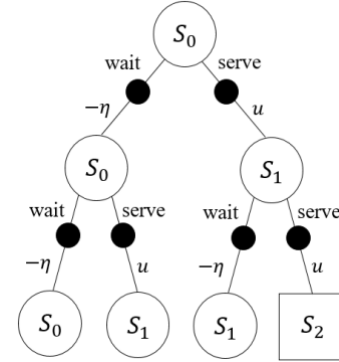


Fig. 3. The first 3 levels of backup diagram for the IH MDP with $N = 2$. States are labeled by S_n where n is the number of filled slots.

B. Finite-Horizon MDP

Unlike the IH formulation, in FH MDP, the value of time is expressed by a hard constraint T_f on the termination time. Accordingly, the terminal state is the state when the termination time T_f is reached or the state at which all the N slots are occupied earlier. The state of FN in the FH case is denoted by $S \in \{S_{t,n}\}$, where t and n represent the time and the number of occupied slots, respectively. Like the IH case, we start at $t = 0$ with all slots available, thus the initial state is $S_{0,0}$. However, unlike IH which has only one terminal state, the FH MDP has multiple terminal states. All the FN states $\{S_{T_f,n}; n = 0, 1, \dots, N\}$ and $\{S_{t,N}; t = N, N + 1, \dots, T_f\}$ are terminal states. For instance, consider the example in the IH case with $N = 2$, but now with a strict constraint to terminate within $T_f = 3$. The state transition graph for this FH MDP problem is shown in Fig. 4. There are four terminal states, $S_{3,0}$, $S_{3,1}$, $S_{3,2}$ and $S_{2,2}$. The return G_t in the FH case is limited by the

termination time T_f , $G_t = \sum_{j=0}^{T-1} \gamma^j r_{t+j+1}$. For instance, if the FN terminates at $S_{3,2}$, then the return from initial state is given by $G_0 = r_1 + \gamma r_2 + \gamma^2 r_3$. The FN may have two different episodes from $S_{0,0}$ to $S_{3,2}$ depending on its actions. One episode is $S_{0,0} \rightarrow S_{1,1} \rightarrow S_{2,1} \rightarrow S_{3,2}$, with a corresponding return $G_0 = u_1 + \gamma(\gamma u_3 - \eta)$. And the other episode is $S_{0,0} \rightarrow S_{1,0} \rightarrow S_{2,1} \rightarrow S_{3,2}$ with a return $G_0 = \gamma(u_2 + \gamma u_3) - \eta$. Note that u_2 is referred to the cloud in the first episode, and u_1 is referred to the cloud in the second episode.

The Bellman expectation equations in (1) and (2) hold for the FH case. The value of state $S_{0,0}$ is the expected return considering all dynamics and episodes, i.e., $V(S_{0,0}) = E[G_0]$.

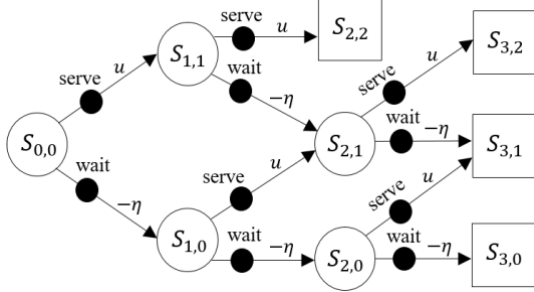


Fig. 4. State transition graph for FH MDP with $N = 2$ and $T = 3$, states are labeled by $S_{t,n}$ where t is the time and n is the number of filled slots.

The objective of the FN in both IH and FH MDP is to utilize the N resource slots for high priority IoT applications in a timely manner. This can be done through maximizing the value of initial state $V(S_0)$. To achieve this objective, an optimal decision policy is required, which is discussed in the following section.

IV. OPTIMAL POLICIES

A decision-making policy can be defined as the set of probabilities of taking a particular action given the state, i.e., $\pi = P(a|S)$ for all possible state-action pairs. The policy π is said to be optimal if it maximizes the value of all states, i.e., $\pi^* = \arg \max_{\pi} V_{\pi}(S), \forall S$. Hence, to find the optimal policy we need to find the optimal state-value function $V^*(S) = \max_{\pi} V_{\pi}(S)$, which selects the best action at each state. Defining the optimal action-value function $Q^*(S, a) = \max_{\pi} Q_{\pi}(S, a)$, from (1) and (2), we can write the optimal state-value function as,

$$V^*(S) = \max_a Q^*(S, a) = \max_a E[r_{t+1} + \gamma V^*(S') | S, a]. \quad (3)$$

The notion of optimal state-value function $V^*(S)$ is greatly simplifies the search for optimal policy. Since the goal of maximizing the expected future rewards is already taken care of the optimal value of the successor state, $V^*(S')$ can be taken out of the expectation in (3). Hence, the optimal policy is given by the best local actions at each state,

$$a^* = \arg \max_a E[r_{t+1} | S, a] + \gamma V^*(S' | S, a). \quad (4)$$

This solution approach is known as Dynamic Programming (DP).

A. Optimum Policy for the IH MDP Problem

In our problem, first the user arrives, then we make a decision to serve or wait (refer to the cloud), meaning that the reward u for serving and the reward $-\eta$ for waiting are known at the time of decision making. Thus, from (4), the optimal action at state S_n given by

$$a_n^* = \begin{cases} \text{serve if } u + \gamma V^*(S_{n+1}) > -\eta + \gamma V^*(S_n), \\ \text{wait otherwise,} \end{cases} \quad (5)$$

for $n = 1, \dots, N$, where $V^*(S_N) = 0$. Hence, the optimal decision rule is a thresholding on u for both states, e.g.,

$$a_n^* = \begin{cases} \text{serve if } u > h_n, \\ \text{wait otherwise,} \end{cases} \quad (6)$$

where $h_n = -\eta + \gamma [V^*(S_n) - V^*(S_{n+1})]$ denotes the optimal threshold at state S_n . The optimal state values, required by the optimal policy as shown in (6), can be computed through the value iteration technique. The procedure to learn the optimal policy from the IoT environment using Monte Carlo simulations is given in Algorithm 1.

ALGORITHM 1: LEARNING OPTIMUM POLICY FOR IH MDP

- 1: Select γ, η ;
 - 2: Initialization: $V(S) \leftarrow 0$ for all S
 - 3: $Returns(S)$: an array to save states' returns in all iterations
 - 4: **for** iteration = 1, 2, ... **do**
 - 5: Generate an episode: Take actions using (6) until termination
 - 6: $G(S) \leftarrow$ sum of discounted rewards from S till terminal state for all states appearing in the episode
 - 7: Append $G(S)$ to $Returns(S)$
 - 8: $V(S) \leftarrow average(Returns(S))$
 - 9: **if** $V(S)$ converge for all S **then**
 - 10: **break**
 - 11: **end if**
 - 12: **end for**
 - 13: Use $V(S)$ to find optimal actions using (6)
-

Given the design parameters η and γ , and the data $\{u_t\}$, Algorithm 1 shows how to learn the optimal policy for IH MDP. Note that $\{u_t\}$ can be real data from the IoT environment, as well as from simulations if the probability distribution is known. At line 2, we initialize all state values with zeros. The $Returns$ array at line 3 represents a matrix to save the return of each state at every episode, which corresponds to an iteration. In each iteration, the current state values, which constitutes the current policy, are used to take actions until the terminal state is reached. To promote exploring different states randomized actions can be taken sometimes at line 6 [32]. $G(S)$ in line 7 represents a vector of returns of all states appearing in the episode. Inserting these values into the $Returns$ array the state values are updated by taking the average as shown in lines 8 and 9. The algorithm stops when all state values converge, the converged values are then used to determine actions as in (6).

B. Optimum Policy for the FH MDP Problem

Similar to IH MDP (cf. (6)), from (4), we can show that the optimal policy in FH MDP is defined by the optimal decision thresholds $\{h_{t,n}\}$ at each state $S_{t,n}$ as follows

$$a_{t,n}^* = \begin{cases} \text{serve if } u > h_{t,n}, \\ \text{wait otherwise,} \end{cases} \quad (7)$$

where $h_{t,n} = \gamma [V^*(S_{t+1,n}) - V^*(S_{t+1,n+1})] - \eta$, since the number of states is finite in the FH case, we can use the backward induction technique to compute the optimal thresholds $\{h_{t,n}\}$ assuming some training data $\{u_t\}$ is available to learn some key statistics of the IoT environment. Starting with the terminal states, which have value zero, we can compute the optimal state values and consequently the optimal thresholds for all states by moving backwards. Actually, we only need to compute the optimal thresholds for a subset of all states. Firstly, note that not all states $\{S_{t,n}\}$ are accessible for all t and n . Even if one slot

is filled at each t , the states with $n > t$ are not accessible, as shown in Fig. 5.

	$n=0$	$n=1$	$n=2$...	$n=T_f-N$...	$n=N-1$	$n=N$
$t=0$	V, h							
$t=1$	V, h	V, h						
$t=2$	V, h	V, h	V, h					
\vdots	\vdots	\vdots	\vdots	\vdots				
$t=T_f-N$	$V=E[u], h=0$	V, h	V, h	...	V, h			
\vdots	\vdots	\vdots	\vdots	\vdots	\vdots	\vdots		
$t=N-1$	$V=E[u], h=0$	$V=E[u], h=0$	$V=E[u], h=0$...	V, h	...	V, h	
$t=N$	$V=E[u], h=0$	$V=E[u], h=0$	$V=E[u], h=0$...	V, h	...	V, h	$V=0$
\vdots	\vdots	\vdots	\vdots	\vdots	\vdots	\vdots	\vdots	\vdots
$t=T_f-2$	$V=E[u], h=0$	$V=E[u], h=0$	$V=E[u], h=0$...	$V=E[u], h=0$...	$V, h=\gamma E[u]-\eta$	$V=0$
$t=T_f-1$	$V=E[u], h=0$	$V=E[u], h=0$	$V=E[u], h=0$...	$V=E[u], h=0$...	$V=E[u], h=0$	$V=0$
$t=T_f$	$V=0$	$V=0$	$V=0$...	$V=0$...	$V=0$	$V=0$

Fig. 5. FH state values and thresholds that need to be computed via backward induction (green diagonal band). Start with the farthest state $S_{T_f-2, N-1}$ (checked green box) and traverse backwards the diagonal band until the initial state $S_{0,0}$ (see Algorithm 2). The terminal states (dark gray), the trivial states whose optimal action is always *serve* (light gray), and the not accessible states (red dotted) are also shown.

Secondly, note that there are $T_f + 1$ terminal states with value zero ($T_f + N$ from early stopping with $T < T_f$ and $N + 1$ from $T = T_f$, $n = 0, 1, \dots, N$), which do not require threshold, as shown with dark gray in Fig. 5. Next, note that for all the non-terminal states at time $T_f - 1$, both *serve* and *wait* actions result in a terminal state with zero value, thus the decision is made based on only the immediate rewards (u vs. $-\eta$). That is, at those states the optimal action is always *serve*, hence the threshold on u is zero and the state value is $E[u]$, as shown in Fig. 5. Similarly, for $t = T_f - N, \dots, T_f - 2$, there is a number of non-terminal states for which both actions yield the same future value, hence have zero threshold and value $E[u]$. Specifically, the states $\{S_{t,n}; t = T_f - l, n = 0, \dots, N - l, l = 1, \dots, N\}$ have state value $E[u]$ and threshold 0, as shown with light gray in Fig. 5.

Finally, for the $(T_f - N)N$ remaining states in a diagonal band, shown with green in Fig. 5, the state values and the corresponding thresholds need to be computed backwards starting with the farthest state $S_{T_f-2, N-1}$ from the initial state $S_{0,0}$. The total reward is u if served, whereas it is $\gamma E[u] - \eta$ if waited, giving the threshold $h_{T_f-2, N-1} = \gamma E[u] - \eta$, as shown by the checked green box in Fig. 5. Then, its state value is written as

$$V(S_{T_f-2, N-1}) = P(u > h_{T_f-2, N-1}) E[u | u > h_{T_f-2, N-1}] + \{1 - P(u > h_{T_f-2, N-1})\} \{\gamma E[u] - \eta\}. \quad (8)$$

where the first and second terms correspond to the *serve* and *wait* actions, respectively. Note that the probability $P(u > h_{T_f-2, N-1})$ and the expectation $E[u | u > h_{T_f-2, N-1}]$ can be computed through some observations $\{u\}$ from the IoT environment. With $V(S_{T_f-2, N-1})$ computed, we can now find the threshold for the two undiscovered neighboring states above it, namely $S_{T_f-3, N-2}$ and $S_{T_f-3, N-1}$ using

$$h_{t,n} = -\eta + \gamma[V^*(S_{t+1,n}) - V^*(S_{t+1,n+1})], \quad (9)$$

from (7). Then, using the thresholds the state values are computed similarly to (8) as follows

$$V(S_{t,n}) = P(u > h_{t,n}) \{E[u | u > h_{t,n}] + \gamma V(S_{t+1, n+1})\} + \{1 - P(u > h_{t,n})\} \{\gamma V(S_{t+1, n}) - \eta\}. \quad (10)$$

In the same way, by computing first the threshold and then the state value via (9) and (10), respectively, the remaining states in the diagonal band are traversed backwards until the initial state $S_{0,0}$. The key statistics $P(u > h_{t,n})$ and $E[u | u > h_{t,n}]$ are to be found from the IoT environment. The procedure for finding the optimal policy is summarized in Algorithm 2, where by default the terminal states have zero value and $x: -1: y$ denotes the decrement by 1 from x to y . For notational simplicity, the trivial states are also included in the loops at lines 2 and 3. The range for the loops can be modified to exclude the trivial states.

ALGORITHM 2: LEARNING OPTIMUM POLICY FOR FH MDP

- 1: Select γ, η
 - 2: **for** $i = N - 1: -1: 0$ **do**
 - 3: **for** $j = T_f - 1: -1: i$ **do**
 - 4: $h_{j,i} = \gamma[V(S_{j+1,i}) - V(S_{j+1,i+1})] - \eta$
 - 5: Compute $a \leftarrow E[u | u > h_{j,i}]$ and $p \leftarrow P(u > h_{j,i})$
 - 6: $V(S_{j,i}) = p\{a + \gamma V(S_{j+1,i+1})\} + (1 - p)\{\gamma V(S_{j+1,i}) - \eta\}$
 - 7: **end for**
 - 8: **end for**
 - 9: Return $\{h_{j,i}\}$
-

V. SIMULATIONS

We next provide simulation results to compare the performance of the FN when implementing the RL-based algorithms, given in Algorithms 1 and 2, with the FN performance when a fixed thresholding algorithm is employed. Our simulations consider both cases: when FN is under soft and hard time constraints represented by the IH and FH formulations, respectively. We consider that the FN is empowered with computing and storage resources of five slots, i.e., $N = 5$. We evaluate the performances in various IoT environments with different compositions of latency requirements. Specifically, we

consider 10 utility classes with different latency requirements to exemplify the variety of IoT applications in an F-RAN setting. By changing the composition of utility classes, we generate 19 scenarios, 6 of which are summarized in Table 2. Higher percentages of high-utility users make the IoT environment richer.

TABLE 2
STATISTICS OF VARIOUS IOT ENVIRONMENTS

	φ_1	φ_4	φ_7	φ_{10}	φ_{15}	φ_{19}
P(u = 1)	0.015	0.012	0.01	0.008	0.004	0.001
P(u = 2)	0.073	0.062	0.05	0.038	0.019	0.004
P(u = 3)	0.365	0.308	0.25	0.192	0.096	0.019
P(u = 4)	0.292	0.246	0.2	0.154	0.077	0.015
P(u = 5)	0.205	0.172	0.14	0.108	0.054	0.011
P(u = 6)	0.014	0.057	0.1	0.142	0.214	0.271
P(u = 7)	0.013	0.051	0.09	0.129	0.193	0.244
P(u = 8)	0.011	0.046	0.08	0.114	0.171	0.217
P(u = 9)	0.009	0.034	0.06	0.086	0.129	0.163
P(u = 10)	0.003	0.012	0.02	0.029	0.043	0.055
$\rho = P(u > 5)$	5%	20%	35%	50%	75%	95%
E[u]	3.82	4.4	4.97	5.55	6.5	7.27

Denoting an IoT environment of particular statistics with φ , in Table 2 we show the statistics of $\varphi_1, \varphi_4, \varphi_7, \varphi_{10}, \varphi_{15}$, and φ_{19} . The last two rows in Table 2 show the probability ρ of utility being greater than 5, and the expected value of u , respectively. The first 10 rows in the table provide detailed information given by the probability of each utility value in an IoT environment. In the considered 19 scenarios, ρ increases by 0.05 from 5% to 95% for $\varphi_1, \varphi_2, \dots, \varphi_{19}$ respectively. The remaining 13 scenarios have statistics proportional to their ρ values. We started with a general scenario given by φ_7 for the following IoT applications: smart farming, smart retail, smart home, wearables, entertainment, smart grid, smart city, industrial Internet, autonomous vehicles, and connected health, which correspond to the utility values 1, 2, ..., 10, respectively. Then, we changed ρ to obtain the other scenarios.

A. Infinite Horizon

We firstly consider the IH formulation for the IoT environment given by scenario φ_7 and an FN with 5 slots of resources. Fig. 6 shows how the FN learns the optimal policy using Algorithm 1 with $\eta = 1$ and $\gamma = 1$.

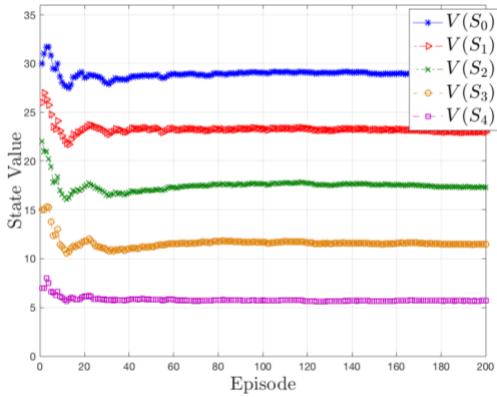


Fig. 6. Learning optimum policy of IH MDP, with $N = 5$, $\eta = 1$ and $\gamma = 1$, by applying RL algorithm given by Algorithm 1 to obtain the optimal state values.

By interaction with the environment, the FN updates the state value functions which converge to the optimum policy. From Fig. 6, the optimal state values $V^*(S_0), V^*(S_1), V^*(S_2), V^*(S_3), V^*(S_4)$, are

28.61, 22.89, 17.27, 11.53, and 5.84 respectively, hence from (6) the corresponding decision thresholds are 4.72, 4.62, 4.74, 4.69, and 4.84. Note that the optimal policy is learned quickly as the state values converge after around 50 episodes.

As shown in Figs. 7, 8, and 9, we test the effect of changing η and γ on the FN performance when applying Algorithm 1 in IH MDP with φ_7 . We consider $\gamma \in \{0, 0.1, 0.2, \dots, 1\}$ and $\eta \in \{0, 1, 2, \dots, 10\}$. The average total served utility for various combinations of η and γ is shown in Fig. 7. Putting less weight for future rewards represented by smaller γ , the FN is encouraged to serve regardless of the penalty. It maintains an average total served utility of about 24.85, which is about five times the expected utility given in Table 2 due to the available 5 slots of resources. The corresponding average termination time is 5 as shown in Fig. 8. Similar results of average total served utility and expected termination time are experienced for large waiting penalty η irrespective of γ since serving is encouraged also in this case. The average total served utility increases to about 33.8 for $\gamma = 1$ and $\eta = 1$, with a corresponding T of about 10.27. A maximum average total served utility of 50 is achieved when $\eta = 0$ and $\gamma = 1$ as there is no penalty of waiting with maximum weight for future rewards. In this case, the FN waits too long to serve the maximum utility ($u = 10$) users, hence T exceeds 200 as shown in Fig. 8.

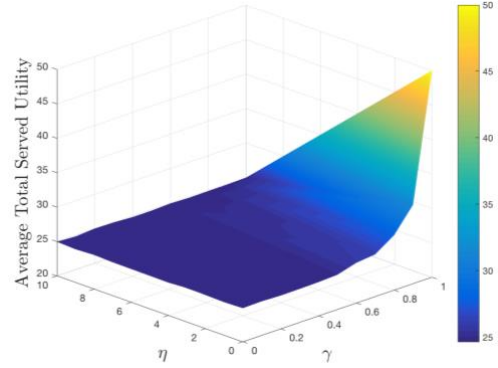


Fig. 7. The average total served utilities by FN with $N = 5$ when applying Algorithm 1 for different combinations of η and γ in IH MDP.

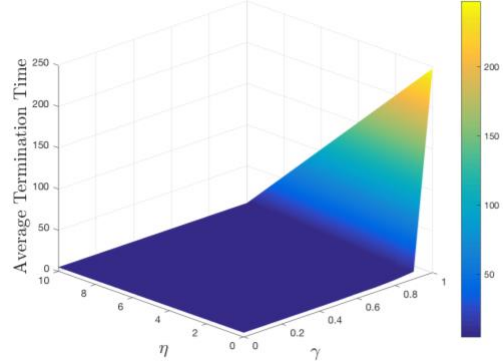


Fig. 8. Average termination time from the initial state for FN with $N = 5$ when applying Algorithm 1 for different combinations of η and γ in IH MDP.

Recall that the FN objective is to maximize the expected total served utility and minimize the expected termination time. Hence, to compare the performance of Algorithm 1 with the fixed threshold algorithm, which does not learn from the interactions with environment, we define an objective performance metric R as shown in (11).

$$R = E \left[\sum_{m=1}^M u_m - \theta(T - M) \right], \quad (11)$$

where a served utility is denoted with u_m , the penalty for waiting is denoted with θ , and the number of served utilities in an episode is denoted with M . For any policy, this metric makes sense since it measures the average performance in terms of a meaningful objective. In the proposed RL algorithm with $\eta = \theta$ and $\gamma = 1$, R corresponds to the average return, $E[G|S = S_0]$. Fig. 9 shows the effect of η and γ on the average return. Note that for $\eta = 0$, there is no penalty for T in $E[G|S = S_0]$, achieving a maximum value of 50 when $\gamma = 1$.

We compare the performance of the proposed RL algorithm with the fixed-threshold algorithm, which uses the same threshold regardless of the environment, in the 19 IoT environments in IH MDP in terms of R with $\theta = 1$. For the RL algorithm, we consider the design parameters $\eta = 1$ and $\gamma = 1$, and for the fixed threshold algorithm we consider all possible thresholds 1, 2, ..., 10.

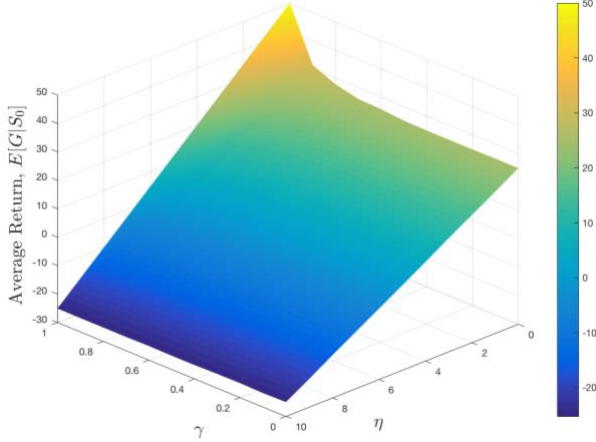


Fig. 9. The average return $E[G|S = S_0]$ for FN with $N = 5$ when applying Algorithm 1 for different combinations of η and γ in IH MDP.

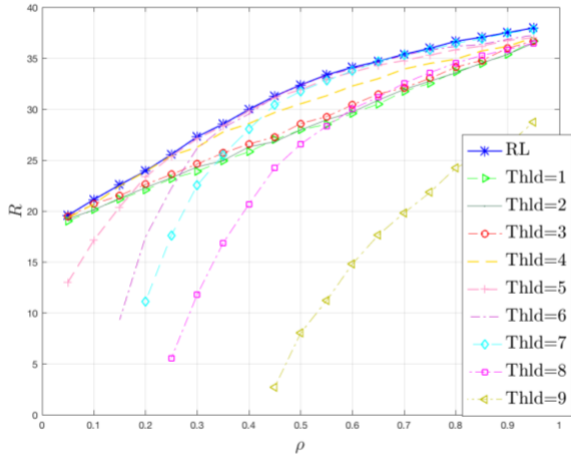


Fig. 10. Performance of FN with $N = 5$ in various IoT environments when applying Algorithm 1 with $\eta = 1$, $\gamma = 1$, and the fixed-threshold algorithm with different thresholds.

As shown in Figs. 10 and 11, the RL algorithm exhibits the best performance as it adaptively learns how to balance early termination with higher utilities. It never terminates too early or too late ($T \approx 5$ for all environments as seen in Fig. 11), as opposed to the fixed-threshold algorithm which is not adaptive to the environment. As seen Fig. 10, the performance of fixed-threshold algorithm with thresholds 1, 2, 3, 8, 9 are steadily below that of the RL algorithm. Threshold 4 has a comparable performance to RL for the environments with $\rho \leq 25\%$, after which its performance starts to decline. Although thresholds 5, 6, 7 have good performances close to RL for environments with medium to high ρ , they perform far from RL for IoT environments with small

ρ . The R values for threshold 10 are negative for all environments due to the long termination time which exceeds 90, thus it does not appear in Figs. 10 and 11.

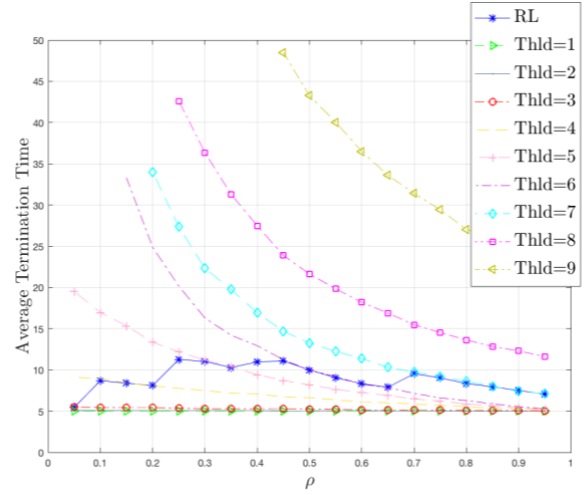


Fig. 11. The average termination time for FN with $N = 5$ in various IoT environments when applying Algorithm 1 with $\eta = 1$, $\gamma = 1$, and the fixed-threshold algorithm with different thresholds.

B. Finite Horizon

In the FH case, we consider the same objective performance metric given in (11) to compare the performance of the FN with $N = 5$ when applying the proposed RL algorithm (Algorithm 2) with the fixed-threshold algorithm. We consider a finite horizon of $T_f = 10$, which serves as a strict termination time. Since we already have a time constraint on the FN which represents the value of time, we consider $\eta = \theta = 0$. As shown in Fig. 12, RL algorithm adaptively learns how to achieve the objective for all IoT environments under a strict termination time constraint. Similar to the IH case, RL algorithm dominates the fixed-threshold algorithm for all IoT environments. Another significant advantage of the proposed RL algorithms is that they learn the optimal thresholds from the environment. On the other hand, the fixed-threshold algorithm cannot automatically select the best threshold for the environment. Similar discussions as discussed in Figs. 6-9 for the IH case apply also the FH case, hence we do not present them here for brevity.

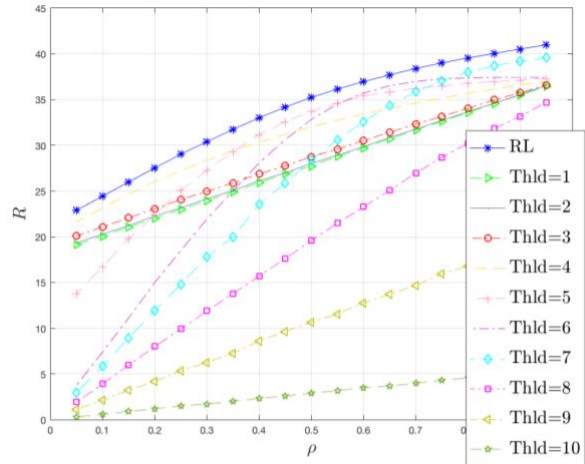


Fig. 12. Performance of FN with $N = 5$ in FH MDP with $T_f = 10$ in various IoT environments when applying Algorithm 2 with $\eta = 0$, $\gamma = 1$, and the fixed-threshold algorithm with different thresholds.

VI. CONCLUSIONS

We formulated the resource allocation problem for F-RAN in a heterogeneous IoT environment as a Markov Decision Process (MDP) problem in two ways, the infinite-horizon (IH) and finite-horizon (FH) formulations. Then, we provided the optimum solutions (decision policies) for the IH and FH problems. Various IoT environments were considered in the simulations to test the performance of the proposed RL-based algorithms. The numerical results corroborated the fact that RL methods adapt to the environment by learning the optimum policy from experience. We showed that the proposed RL methods always outperforms the fixed-threshold method, which does not learn from the environment, irrespective of the IoT environment and the termination time constraint (i.e., IH or FH formulation). Moreover, the fixed-threshold algorithm cannot automatically select the best threshold for the environment.

REFERENCES

- [1] Cisco, "Cisco Visual Networking Index: Global Mobile Data Traffic Forecast Update, 2016–2021," White Paper, [Online]. Available: <https://www.cisco.com/c/en/us/solutions/collateral/service-provider/visual-networking-index-vni/mobile-white-paper-c11-520862.html>.
- [2] A. T. Nassar, A. I. Sulyman, and A. Alsanie, "Achievable RF Coverage and System Capacity Using Millimeter Wave Cellular Technologies in 5G Networks," Proc. IEEE-CCECE 2014, Toronto, Canada, May 2014.
- [3] A. I. Sulyman, A. T. Nassar, M. K. Samimi, G. R. MacCartney Jr., T. S. Rappaport, and A. Alsanie, "Radio propagation path loss models for 5G cellular networks in the 28 and 38GHz millimeter wave bands," *IEEE Communications Magazine*, vol. 52, no. 9, pp. 78–86, 2014.
- [4] S. Rangan, T. S. Rappaport, and E. Erkip, "Millimeter-Wave Cellular Wireless Networks: Potentials and Challenges," *Proc. IEEE*, vol. 102, no. 3, Mar. 2014, pp. 366–86.
- [5] J. Zhang et al., "3D MIMO for 5G NR: Several Observations from 32 to Massive 256 Antennas Based on Channel Measurement," *IEEE Communications Magazine*, vol. 56, issue. 3, pp. 62-70, 2018.
- [6] B. Yang et al., "Digital Beamforming-Based Massive MIMO Transceiver for 5G Millimeter-Wave Communications," *IEEE Early Access Articles*, pp. 1-16, 2018.
- [7] S. H. Park, O. Simeone and S. Shamai Shitz, "Joint Optimization of Cloud and Edge Processing for Fog Radio Access Networks," *IEEE Trans. Wireless Commun.*, vol. 15, no. 11, pp. 7621-7632, Nov. 2016.
- [8] M. Peng, Y. Sun, X. Li, Z. Mao and C. Wang, "Recent Advances in Cloud Radio Access Networks: System Architectures, Key Techniques, and Open Issues," *IEEE Communications Surveys & Tutorials*, vol. 18, no. 3, pp. 2282-2308, thirdquarter 2016.
- [9] Z. Zhao et al., "Cluster Content Caching: An Energy-Efficient Approach to Improve Quality of Service in Cloud Radio Access Networks," *IEEE JSAC*, vol. 34, no. 5, pp. 1207-21, May. 2016.
- [10] M. Peng, C. Wang, V. Lau and H. V. Poor, "Fronthaul-constrained cloud radio access networks: insights and challenges," *IEEE Wireless Communications*, vol. 22, no. 2, pp. 152-160, Apr. 2015.
- [11] W. Wang, V. K. N. Lau and M. Peng, "Delay-Aware Uplink Fronthaul Allocation in Cloud Radio Access Networks," *IEEE Transactions on Wireless Communications*, vol. 16, no. 7, pp. 4275-4287, July 2017.
- [12] S. Wang, X. Zhang, Y. Zhang, et al., "A survey on mobile edge networks: Convergence of computing, caching and communications," *IEEE Access*, vol. 5, pp. 6757 - 6779, Mar. 2017.
- [13] Y. Y. Shih, W. H. Chung, A. C. Pang, T. C. Chiu and H. Y. Wei, "Enabling Low-Latency Applications in Fog-Radio Access Networks," *IEEE Network*, vol. 31, no. 1, pp. 52-58, Jan/Feb. 2017.
- [14] G. Fettweis, "The Tactile Internet: Applications and Challenges," *IEEE Vehicular Technology Magazine*, vol. 9, issue. 1, pp. 64-70, 2014.
- [15] Q. Zheng et al., "Delay-Optimal Virtualized Radio Resource Scheduling in Software-Defined Vehicular Networks via Stochastic Learning," *IEEE Trans. Vehic. Tech.*, vol. 65, no. 10, Oct. 2016, pp. 7857–67.
- [16] P. Schulz, et al., "Latency critical IoT applications in 5G: Perspective on the design of radio interface and network architecture," *IEEE Commun. Mag.*, vol.55, no. 2, pp. 70–78, Feb. 2017.
- [17] Y. Sahnı, J. Cao, S. Zhang, and L. Yang, "Edge mesh: A new paradigm to enable distributed intelligence in Internet of Things," *IEEE Access*, vol. 5, pp. 16441–16458, 2017.
- [18] A. Pang, W. Chung, T. Chiu, and J. Zhang, "Latency-Driven Cooperative Task Computing in Multi-user Fog-Radio Access Networks," *2017 IEEE 37th International Conference on Distributed Computing Systems (ICDCS)*, pp. 615–624, 2017.
- [19] G. M. Shafiqur Rahman, M. Peng, K. Zhang, and S. Chen, "Radio Resource Allocation for Achieving UltraLow Latency in Fog Radio Access Networks," *IEEE Access*, vol. 6, pp. 17442–17454, 2018.
- [20] J. Oueis, E. C. Strinati and S. Barbarossa, "The Fog Balancing: Load Distribution for Small Cell Cloud Computing," *2015 IEEE 81st Vehicular Technology Conference - Spring, Glasgow, 2015*, pp. 1-6.
- [21] T. C. Chiu, W. H. Chung, A. C. Pang, Y. J. Yu and P. H. Yen, "Ultra low latency service provision in 5G fog-radio access networks", in Proc. *IEEE 27th Annual International Symposium in Personal, Indoor, and Mobile Radio Communications*, 2016, pp. 1-6.
- [22] S. H. Park, O. Simeone and S. Shamai Shitz, "Joint Optimization of Cloud and Edge Processing for Fog Radio Access Networks," *IEEE Trans. Wireless Commun.*, vol. 15, no. 11, pp. 7621-7632, Nov. 2016.
- [23] T. Gao, M. Chen, H. Gu, and C. Yin, "Reinforcement Learning based Resource Allocation in Cache-Enabled Small Cell Networks with Mobile Users," *2017 IEEE/CIC International Conference on Communications in China (ICCC)*, 2017, pp. 1-6.
- [24] D. Vu, N. Dao, and S. Cho, "Downlink Sum-Rate Optimization Leveraging Hungarian Method in Fog Radio Access Networks," *2018 International Conference on Information Networking (ICOIN)*, 2018, pp. 56-60.
- [25] Y. Liu; S. Cheng, and Y. Hsueh, "eNB Selection for Machine Type Communications Using Reinforcement Learning Based Markov Decision Process," *IEEE Transactions on Vehicular Technology*, vol. 66, issue: 12, pp. 11330-11338, 2017.
- [26] M. Condoluci, T. Mahmoodi, E. Steinbach, and M. Dohler, "Soft Resource Reservation for Low-Delayed Teleoperation Over Mobile Networks," *IEEE Access*, vol. 5, pp. 10445-10455, 2017.
- [27] H. Name, F. Oladipo, and E. Ariwa, "User Mobility and Resource Scheduling and Management in Fog Computing to Support IoT Devices," *2017 Seventh International Conference on Innovative Computing Technology (INTECH)*, 2017, pp. 191-196.
- [28] M. Peng et. al., "Recent Advances in Fog Radio Access Networks: Performance Analysis and Radio Resource Allocation," *IEEE Access*, vol. 4, pp. 5003-5009, 2016.
- [29] T. Park, N. Abuzainab, and W. Saad, "Learning how to communicate in the Internet of Things: Finite resources and heterogeneity," *IEEE Access*, vol. 4, pp. 7063–7073, 2016.
- [30] M. Yan, G. Feng, and S. Qin, "Multi-RAT Access based on Multi-Agent Reinforcement Learning," *GLOBECOM 2017 - 2017 IEEE Global Communications Conference*, 2017, pp. 1-6.
- [31] Y. Wei, F. Yu, M. Song, and Z. Han, "User Scheduling and Resource Allocation in HetNets With Hybrid Energy Supply: An Actor-Critic Reinforcement Learning Approach," *IEEE Transactions on Wireless Communications*, vol. 17, Issue: 1, pp. 680-692, 2018.
- [32] R. Sutton and A. Barto, *Reinforcement Learning: An Introduction*. Cambridge, MA, USA: MIT Press, 1998.